Stroke-Volume-Allocation Model Enabling Wearable Sensors for Vascular Age and Cardiovascular Disease Assessment

Shirong Qiu[1], Bryan PY Yan[2], Ni Zhao[1*]

[1]The Department of Electronic Engineering, The Chinese University of Hong Kong, Hong Kong SAR

[2]The Division of Cardiology, Department of Medicine and Therapeutics, The Chinese University of Hong Kong, Hong Kong SAR

([*]Corresponding author: Ni Zhao. Email: nzhao@ee.cuhk.edu.hk)

Supplementary Notes

Supplementary note 1: Analysis of arterial wall stiffening

In the experimental observations, the Young's modulus of the elastin fiber E_e (1.5-4.1×10^6 dynes/cm^2) is much smaller than collagen fiber E_c[1] (0.3-2.5×10^{10} dynes/cm^2). The composite Young's modulus of the artery E, by the rule of mixtures, can be expressed as

$$E = E_c \cdot x_c + E_e \cdot x_e + \zeta \tag{1}$$

where x_c and x_e are the volume fraction of the elastin fibers and collagen fibers, respectively. And $x_c = 1 - x_e$. ζ is the constant contribution from vascular smooth muscle. Based on the mechanical analysis of elastic vessel[2],

$$\frac{r - r_0}{r_0} = \frac{(P_{in} - P_{out}) \cdot r_0}{E \cdot h} \tag{2}$$

where P_{in} is the intravascular wall pressure; P_{out} is the extravascular wall pressure; r_0 is vascular radius in the natural state. r is vascular radius under transmural pressure. h is vessel wall thickness. By combining Supplementary Equation (1) & (2),

$$r = \frac{(P_{in} - P_{out}) \cdot r_0^2}{E \cdot h} + r_0 = \frac{(P_{in} - P_{out}) \cdot r_0^2}{[x_e \cdot (E_e - E_c) + E_c + \zeta] \cdot h} + r_0 \tag{3}$$

when r_0, $P_{in} - P_{out}$ and h are fixed, we have

$$r \propto \frac{1}{E} \tag{4}$$

Based on Supplementary Equation (2), the arterial stiffness respective to r and can be expressed as[1]

$$Stiffness_r = \frac{dP}{dr} = \frac{Eh}{r_0^2} \propto E \tag{5}$$

Let the elastic proportion of the aorta (EPA) is expressed as the ratio of elastin fibers and collagen fibers, i.e.,

$$EPA = \frac{x_e}{x_c} \tag{6}$$

From Supplementary Equation (3) the radius r is proportional to EPA when the other parameters are fixed. For the elastic artery, the EPA in the elastic aorta (E) is larger than the stiff (S) artery which alter the cushioning function of the aorta and the modules, i.e.,

$$\begin{aligned} & EPA_E(x_c \downarrow, x_e \uparrow) > EPA_S(x_c \uparrow, x_e \downarrow) \\ & \xrightarrow{(S.1)} E_E < E_S \\ & \xrightarrow{(S.5)} Stiffness_{r,E} < Stiffness_{r,S} \\ & \xrightarrow{(S.4)} r_E > r_S \\ & \longrightarrow Buffering\ Vol_E > Buffering\ Vol_S \end{aligned} \tag{7}$$

The last term in Supplementary Equation (7) is due to the fact that an elastic artery will induce a greater expansion radius, leading to an increased capacity for arterial blood volume storage. Since the younger (Y) with elastic aorta with higher fraction of elastin fibers than the older (O) with stiff aorta[3], the Young's modulus of the elastic aorta E_Y is smaller than the stiff aorta E_O, i.e. $E_Y < E_O$. This is consistent with the study by B. Sonesson et al.[4] which reported that the modulus of elasticity increases with age. Consequently, elderly individuals with a stiff aortic vessel, denoted as E_O, may encounter inadequate buffering or cushioning of their vascular system in comparison to younger individuals with elastic vascular systems, as stated in Supplementary Equation (7).

Supplementary note 2: SVA model

The Windkessel model can be described as the following physical procedure:

In the systole phase of the cardiac cycle ($0 < t < T_s$), the blood volume is pumped from the left ventricle into the aorta. Some blood volume would be stored in the aorta (expressed as compliance C) and remainder would be push into the peripheral capillaries for supporting tissue and organs (expressed as peripheral vascular resistance, R). The initial pressure corresponds to diastolic blood pressure (DBP) and Q_{in} is the input blood flow. The physical process can be described mathematically as follows:

$$\begin{cases} C\dfrac{dP(t)}{dt} + \dfrac{P(t)}{R} = I(t) \\ P(0) = DBP\ (as\ t = 0) \\ I(t) = Q_{in} \end{cases} \tag{8}$$

In the diastole phase ($T_s < t \leq T_c$), the aorta valve is closed, and no blood is pumped to the peripheral vascular artery. The storing volume in the elastic aorta (compliance) is transferred into the peripheral artery and organ during diastolic duration. The initial pressure corresponds to the pressure at the end of aorta valve closed, i.e., dicrotic notch pressure, P_s^{dn} . Hence, this physical procedure could be described as the following

$$\begin{cases} C\frac{dP(t)}{dt} + \frac{P(t)}{R} = I(t) \\ P(T_s) = P_s^{dn}\ (as\ t = T_s) \\ I(t) = 0 \end{cases} \tag{9}$$

where C is arterial compliance, R is the systematic vascular resistance, $I(t)$ is the aortic blood flow, and $P(t)$ is the aortic pressure.

The solution of the Supplementary Equation (9) in the diastolic phase is

$$P(t) = P_s^{dn} \cdot e^{-\frac{t-T_s}{\tau}} \tag{10}$$

where $\tau = RC$ is a time constant.

The stroke volume in the arterial compliance during the systole phase is

$$\begin{aligned} SV_c &= \int_0^{T_s} I_c\,(t)\,dt = C \cdot \int_0^{T_s} \frac{dP}{dt}\,dt \\ &= C \cdot \big(P(T_s) - P(0)\big) = C \cdot (P_s^{dn} - DBP) \\ &= C \cdot \left(e^{\frac{T_c - T_s}{\tau}} - 1\right) \cdot DBP \end{aligned} \tag{11}$$

where $I_c(t)$ is the blood flow that stored in the compliance.

On the other hand, the stroke volume could be expressed as the product of C and pulse pressure (PP), i.e.

$$SV = C \cdot PP \tag{12}$$

Then the stroke-volume allocation could be expressed as

$$SVA = \frac{SV_c}{SV} = \frac{C \cdot \left(e^{\frac{T_c - T_s}{\tau}} - 1\right) \cdot DBP}{C \cdot PP} = \frac{\left(e^{\frac{T_c - T_s}{\tau}} - 1\right) \cdot DBP}{PP} \tag{13}$$

The clinical intuition of SVA is the elastic buffer function of the arteries that regulates the blood volume distribution in a cardiovascular system. The concept is illustrated in

Supplementary Fig.3, where the analogy between a fire engine and a heart-to-artery system is drawn based on the Windkessel model. In the fire engine case (as shown in Supplementary Fig. 3), we have the canal, pump, windkessel, and spout. The canal is the pathway for water flow from source to destination. The pump generates pressure to propel water through the canal, dictating the delivery rate. The windkessel acts as a reservoir, regulating the pressure and accommodating changes in demand. The spout is where water is discharged with force and direction to combat fires effectively. This analogy draws parallels to the arterial system, where the artery is the equivalence of the canal, the heart is the "pump", the arteries' storage capacity is like the capacity of the windkessel, and the blood distribution to peripheral organs and tissues functions like the "spout". It can be seen from this comparison that SVA essentially reflects the arteries' storage-regulated fluid transportation and distribution in an arterial system. In a living body, blood volume is pumped from heart and distributed differently between the elastic arteries and peripheral organs and tissues in each heartbeat to maintain normal body function. Based on this, the SVA here describes the proportion of blood volume that can be stored in the elastic arteries in each heartbeat. Normally, 60% of the blood volume is stored in the elastic arteries during systole (i.e., SVA=60% in Supplementary Fig.3 (a)), and the remaining 40% is ejected for consumption by peripheral organs and tissues. However, when peripheral organs and tissues have a higher demand for blood nutrients, such as during activity, meals, and respiratory changes, more blood volume is allocated to the peripheral arteries, resulting in a lower proportion of blood volume allocated in the elastic arteries, i.e., a lower stroke volume allocation (SVA=40%).

In physiology, SV is the stroke volume, i.e., the amount of blood pumped from the heart per heartbeat. SVA is the fraction of the stroke volume that can be stored in the elastic arteries, such as aorta. To explain the relation between SVA and SV, we further provide circuit model in Supplementary Fig. 3 (b) to describe the windkessel effect in the cardiac circulation, where SVA (SV_c/SV) is the fraction of the input stroke volume (i.e., $SV = \int_0^{T_c} I(t)dt$) that can be stored in the arterial compliance (i.e., $SV_c = \int_0^{T_s} I_c(t)dt$) during the systole.

Supplementary note 3: SVA is equivalent to the ratio of BP area

For the area of the BP during diastolic duration

$$A_d = \int_{T_s}^{T_c} P\,(t)\,dt = \int_{T_s}^{T_c} P_s^{dn} \cdot e^{-\frac{t-T_s}{\tau}}\,dt$$
$$= \tau \cdot DBP\left(e^{\frac{T_c-T_s}{\tau}} - 1\right) \quad (14)$$

The total area of the BP during the heartbeat cycle is

$$A_s + A_d = R \cdot SV = R \cdot C \cdot PP = \tau PP \quad (15)$$

Hence, when multiply R in the Supplementary Equation (13), the stroke volume allocation can be expressed as the ratio of the area of the blood pressure waveform. i.e.

$$\frac{A_d}{A_s + A_d} = \frac{\tau \cdot DBP \cdot \left(e^{\frac{T_c-T_s}{\tau}} - 1\right)}{\tau PP} = \frac{SV_c}{SV} = SVA \quad (16)$$

Supplementary note 4: SVA calculated by the cardiac information and BP values

Based on Supplementary Equation (16), the BP waveform is measurable and provides reference SVA in practice. However, the continuous BP waveform measurement is expensive when compared to the intermittent home-based BP measurement which limited the accuracy of SVA application. To ease the dilemma, we approximate SVA with BP waveform based on limited BP information. In general,

$$MBP = \frac{A_d}{SVA} \cdot \frac{1}{T_c} \triangleq \frac{\kappa \cdot DBP \cdot (T_c - T_s)}{SVA \cdot T_c} \tag{17}$$

where κ is the ratio of the area of diastolic BP curve and rectangular area of DBP in the diastolic duration (pink region in Fig. 2b right). Hence,

$$SVA \triangleq \frac{\kappa \cdot DBP \cdot \left(1 - \frac{T_s}{T_c}\right)}{MBP} = \delta \cdot \left(1 - \frac{T_s}{T_c}\right) \tag{18}$$

where $\delta = \frac{\kappa \cdot DBP}{MBP}$.

For the above equation, the ratio of DBP and MBP is almost a constant in practice, i.e.,

$$\frac{DBP}{MBP} \approx k \tag{19}$$

We plotted the experimentally measured DBP/MBP versus MBP in Supplementary Fig. 4. It can be clearly seen from the figure that the DBP/MBP ratio is nearly a constant with respect to the change of MBP for each subject. Based on this observation, we further provided the theoretical derivation of Supplementary Equation (19) in **Supplementary note 8**.

Hence, based on Supplementary Equation (18) & (19), we can obtain the linear relationship between SVA and Ts/Tc, i.e.,

$$SVA = -\kappa \cdot k \cdot \left(\frac{T_s}{T_c}\right) + \kappa \cdot k \tag{20}$$

From Supplementary Equation (20), the $\frac{T_s}{T_c}$ shows negatively correlated with SVA. κ is nearly to $\frac{DBP}{MBP}$ which can be obtained directly from a snapshot BP measurement.

Because the representative diastolic blood pressure waveform increases and then decreases, the original diastolic blood pressure area can be approximated using the trapezoidal area approximation technique (area compensation minimizes error, as shown in Supplementary Fig. 5).

In practice, by quadrilateral approximation of BP waveform, the SVA can be further expressed as

$$SVA \cong \frac{(DBP + BP_{dn}) \cdot (T_c - T_s)}{MBP \cdot T_c \cdot 2} \tag{21}$$

Then δ can be expressed as

$$\delta \cong \frac{DBP + BP_{dn}}{2 \cdot MBP} \tag{22}$$

where BP_{dn} is the dicrotic notch point of BP.

Furthermore, one could use the empirical MBP to replace the amplitude of dicrotic notch point of BP[5], i.e. $BP_{dn} = MBP$. Then δ is

$$\hat{\delta}_{MBP} \cong \frac{DBP + MBP}{2 \cdot MBP} \tag{23}$$

The error between $\hat{\delta}_{MBP}$ and δ is generated from the difference between BP_{dn} and MBP, we can easily evaluate it as following

$$\epsilon = \frac{\left|\delta - \hat{\delta}_{MBP}\right|}{\delta} = \frac{|BP_{dn} - MBP|}{DBP + BP_{dn}} \tag{24}$$

We evaluated ϵ in a dataset of blood pressure measurements[6] with a mean error $\bar{\epsilon} < 5\%$, which is small and agree with the previous study[5]. To maintain consistent analysis across different data sets, in this study, we used Supplementary Equation (23) to calculate the δ for the datasets with snapshot BP measurements.

Supplementary note 5: SVA along the arterial tree

As the elastic component of the artery decreases with distance from the aorta[7-9], i.e., $x_{e,distal} < x_{e,proximal}$, the Young's modulus in distal artery is larger than the proximal artery , i.e., $E_{distal} > E_{proximal}$, based on the analysis of **Supplementary note 1.** Furthermore, as shown in Supplementary Equation (7), the distinct compositions of elastic fiber along artery may result in a lower buffering volume (i.e., lower SVA) in the peripheral artery than in the central SVA, i.e., $SVA_{distal} < SVA_{proximal}$. Numerous experimental observations have confirmed that the modulus of elasticity undergoes an increase as the distance from the heart increases.[10,11]

Supplementary note 6: SVA for blood pressure estimation

Based on Supplementary Equation (10), (13) and (33), we could derive DBP as

$$DBP = \frac{P_s^{dn} - SVA \cdot b}{SVA(PSR-1)+1} = \frac{b_s^{dn} - SVA \cdot b}{SVA(PSR-1)+1-k_s^{dn}} \tag{25}$$

The last formula in above equation is based on the following observation

$$P_s^{dn} = DBP \cdot k_s^{dn} + b_s^{dn} \tag{26}$$

where P_s^{dn} is the dicrotic notch pressure, k_s^{dn} and b_s^{dn} are the linear coefficients in the linear relationship of DBP and P_s^{dn}.

Similarly, SBP can be expressed as

$$SBP = \frac{b_s' - SVA \cdot b}{SVA(PSR-1)+1-k_s^{dn}} \tag{27}$$

where $b_s' = PSR \cdot b_s^{dn} + b \cdot (1-k_s^{dn})$ is a constant.

Since the DBP and SBP show the same expression of SVA with different coefficients in Supplementary Equation (25) & (27), the BP can be expressed by SVA as

$$BP = \frac{b_s^* - SVA \cdot b}{SVA(PSR-1)+1-k_s^*} \tag{28}$$

where b_s^* and k_s^* are linear coefficients relating DBP and dicrotic notch pressure P_s^{dn}.

Since there are 4 unknown coefficients in Supplementary Equation (28), we can calibrate this model by input at least 4 measurement pairs. In our experimental observations, the higher dynamic range of the measurement pairs help to construct a stable coefficient and then a reliable SVA-BP estimation model is constructed. In addition, we further provide the stability analysis of the coefficient PSR in Supplementary Equation (28) in the **Supplementary note 9.**

Supplementary note 7: Relation of SVA and PWV

In previous analytical model studies[12], the BP is proportional to the quadratic of pulse wave velocity (PWV) which could be expressed as

$$BP = \alpha \cdot PWV^2 + \beta \tag{29}$$

It means that an increase in PWV may correspond to a higher BP value. On the other hand, based on the BP expressed by SVA in Supplementary Equation (28), where an increase in SVA may correspond to a lower BP value, the relationship between SVA and PWV could be expressed is

$$PWV = \sqrt{\left[\frac{b_s^* - SVA \cdot b}{SVA(PSR-1)+1-k_s^*} - \beta\right]/\alpha} \tag{30}$$

where the parameters of Supplementary Equation (30), such as b_s^*, b, PSR, k_s^*, β and α, can be determined by fitting the corresponding observed clinical data. This expression effectively links the cushioning function and conduit function of the arteries.

Apart from this theoretically derived relationship, we also showed a statistically significant negative correlation between cfPWV and SVA in the experimentally measured datasets (in the manuscript Fig. 3(e)). The trends predicted in the theoretical equation and observed experimentally are consistent, although not mathematically equivalent. Therefore, we explored to the use of (1-SVA) as an indicator for the degree of deterioration of the arterial cushioning function with aging and obtained very positive results. Notably, from a physiological point of view, (1-SVA) represents the demand of blood by peripheral organs and tissues during systole that also associates with the corresponding change of PWV (Supplementary Fig. 6, modified from Ref[13,27] with permissions). In other words, SVA reflects the consumption of blood nutrients (e.g., oxygen and required ions) by peripheral organs and tissues during a systolic phase. Thus, the higher the SVA (i.e., the lower the (1-SVA)), the lower the consumption of the peripheral organs, which would place arteries in a relatively relaxed state, thus producing a correspondingly lower cfPWV.

Furthermore, based on the Supplementary formulation (30), the SVA derived cfPWV (i.e., $cfPWV_{SVA}$) and measured cfPWV showed a consistent increasing trend with age in Supplementary Fig. 7.

Supplementary note 8: The ratio of DBP and MBP

$$\frac{DBP}{MBP} = k + \frac{c}{MBP} \approx k \tag{31}$$

The relationship between DBP and MBP is nearly linear as follows

$$DBP = k \cdot MBP + c \tag{32}$$

This could be observed by SBP and DBP relationship[14]

$$SBP = PSR \cdot DBP + b \tag{33}$$

where *PSR* is the pulse stiffening ratio, b is a constant.

Hence, the DBP could be expressed as

$$DBP = \frac{MBP}{\sigma(PSR-1)+1} + \frac{-b}{PSR - 1 + \frac{1}{\sigma}} \tag{34}$$

When $\sigma = \frac{1}{3}$ as the form factor in Supplementary Equation (34) [15], then

$$c = \frac{-b}{PSR - 1 + \frac{1}{\sigma}} = \frac{-b}{PSR + 2} \tag{35}$$

Since $PSR > 1, c < \frac{|b|}{3} \ll MBP$, in general, hence

$$\frac{c}{MBP} \ll \frac{|b|}{3 \cdot MBP} \tag{36}$$

Since b is the intercept of the regression between SBP and DBP which is a small constant, i.e., $|b| \ll MBP$, then

$$\frac{c}{MBP} \xrightarrow{|b| \ll MBP} 0 \tag{37}$$

We further validated Supplementary Equation (31) based on invasive blood pressure measurements collected from an PWH patient and the MIMIC-I dataset, see Supplementary Fig.4.

Supplementary note 9: The stable pulsatile stiffening ratio (PSR) in the circulation

In general, consider a local relationship of pressure and cross-sectional area in an arterial segment[16], shown in Supplementary Fig. 8, which can be described by

$$Pressure = \alpha + \gamma e^{\beta \cdot Area} \tag{38}$$

where α, β, and γ are pressure-independent constants. α is related to intrinsic properties of an artery to remain patent at very low pressures and γ is a scaling factor for the y-intercept. Area is the cross-sectional area of the arterial segment. β is the beta stiffness, which is expressed as

$$\beta = \frac{ln\,[(SBP - \alpha)/(DBP - \alpha)]}{Pulse\ area} \tag{39}$$

where SBP is systolic blood pressure, DBP is diastolic blood pressure, pulse area is arterial cross-sectional area difference between systolic and diastolic phase.

Then the BP components can be expressed as

$$SBP = PSR \cdot DBP + \alpha(1 - PSR) \tag{40}$$

where PSR is

$$PSR = e^{\beta \cdot (Pulse\ area)} \tag{41}$$

Hence, PSR is influenced by β and pulse area. In very short-term, both parameters are stable which contribute to the constant PSR. By considering a dynamic change of β in changing stiffness, as shown in Supplementary Fig. 8, increasing β, i.e., stiffer of artery, corresponds to a smaller pulse area (red line in younger case), while decrease β corresponds to a larger pulse area (gray line in younger case). Hence, it could be known that the PSR tends to be stable due to the existing of trade-off between β and pulse area. Mathematically, the difference between stiffer PSR_S and elastic PSR_E can be expressed as their difference in the logarithmic form, i.e.,

$$\begin{aligned} \ln(PSR_s) - \ln(PSR_E) &= \beta_s \cdot \Delta A_s - \beta_E \cdot \Delta A_E \\ &= (\beta_E + \varepsilon_\beta) \cdot (\Delta A_E - \varepsilon_A) - \beta_E \cdot \Delta A_E \\ &= \varepsilon_\beta \cdot \Delta A_E - \varepsilon_A \cdot \beta_s \\ &= k_1 \cdot \beta_E \cdot \Delta A_E - k_2 \cdot \Delta A_E \cdot \beta_s \\ &< k_1 \cdot \beta_E \cdot \Delta A_E - k_2 \cdot \Delta A_E \cdot \beta_E \\ &= \beta_E \cdot \Delta A_E \cdot (k_1 - k_2) \\ &\to 0 \end{aligned} \tag{42}$$

where $k_1 = \varepsilon_\beta/\beta_E$ and $k_2 = \varepsilon_A/\Delta A_E$ in the above expression. Since $\varepsilon_\beta \ll \beta_E$ and $\varepsilon_A \ll \Delta A_E$, then $k_1 \to 0$ and $k_2 \to 0$ which will lead to the last result, i.e., $\ln(PSR_s) - \ln(PSR_E) \to 0$ and $PSR_s \approx PSR_E$. These results may contribute to the analysis of the stable parameters in the construction of the SVA-BP model.

Supplementary Table 1. Clinical studies to validate SVA with hemodynamic parameters.

ID	BP	BP measurement method	Ts	Ts measurement method	Tc	Ts & Tc measurements method	PWV/PTT	PWV measurement method	Age	Data form	Diagnosis	Authors	Comments
1	Brachial-Cnap	CNAP/ Penaz Volume clamp	LVET	BPW/ECG/PCG/PPG	HP	BPW/ECG/Epidermal/PPG	-	-	29	Case	HTP	Ours	No. 1, sensors demonstration
2	Aortic & radial	Invasive	LVET	BPW	HP	BPW	-	-	49	Case	DM	Ours	No. 1/ Aortic & radial BP
3	Carotid &Brachial	Vicorder/Oscillometric	LVET	ECG/PPG	HP	ECG/PPG	cfPWV	Pressure foot-to-foot	20-90	Case	MI vs. Normal	Ours	No. 34/14, Apple Watch/INTS
4	Brachial-Finometer	Finapres/Penaz Volume clamp	LVET	PPG	HP	PPG	-	-	>65	Case	Elderly	Ours	No. 13, INTS
5	Radial	Invasive	LVET	BPW	HP	BPW	-	-	Avg. 67	Case	Hybrid	Moody et al.[17]	MIMIC-I/No. 9
6	Aortic	Invasive	LVET	BPW	60/HR	BPW	-	-	Avg. 51	Case	VAS	Bache et al.[18]	No. 40
7	Carotid	Plethysmography	LVET	BPW	60/HR	ECG-RRI	-	-	Avg. 22	Case	Normal	Hasegawa et al.[19]	No. 27
8	Aortic	Catheter Invasive	LVET	BPW	60/HR	BPW	-	-	21-64	Case	AI	Luomanmaki et al.[20]	No. 30
9	Brachial	Auscultation	LVET	BPW/ Tonometry	HP	BPW/ Tonometry	cfPWV	Doppler foot-to-foot	Avg. 52	Group	ESRD vs. Normal	London et al. (a)[21]	No. 79/73
10	Brachial	Auscultation	LVET	BPW/ Tonometry	HP	BPW/ Tonometry	cfPWV	Doppler foot-to-foot	Avg. 50	Group	ESRD vs. Normal	London et al. (b)[22]	No. 70/50
11	Brachial	Auscultation	LVET	BPW/ Tonometry	HP	BPW/ Tonometry	cfPWV	Doppler foot-to-foot	Avg. 53	Group	ESRD	London et al. (c)[23]	Drug/ long-term, No. 24
12	Brachial	Auscultation	LVET	BPW/ Tonometry	HP	BPW/ Tonometry	cfPWV	Doppler foot-to-foot	Avg. 47	Group	HPT vs Normal	London et al. (d)[24]	No. 84/84
13	Brachial	Auscultation	LVET	BPW/ Tonometry SphygmoCor	HP	BPW/ Tonometry SphygmoCor	cfPWV	Complior foot-to-foot	Avg. 54	Group	E-HPT vs. Normal	London et al. (e)[25]	No. 147/98

BP: blood pressure; LVET: left ventricular ejection time; Ts: systolic time; Tc: cardiac cycle; BPW: blood pressure waveform; cfPWV: carotid-femoral pulse wave velocity; HP: heart period; ECG: electrocardiogram; PPG: photoplethysmography; Epidermal: epidermal pulse; RRI:R-R interval from ECG signal; MI: myocardial infarction; VAS: valvular aortic stenosis; AI: aortic incompetence; E-HPT: essential hypertension; HPT: hypertension; ESRD: end-stage renal disease; DM: Diabetes mellitus. Brachial-Cnap: reconstructed brachial pulse wave by Cnap; Brachial-Finometer: reconstructed brachial pulse wave by Finometer.

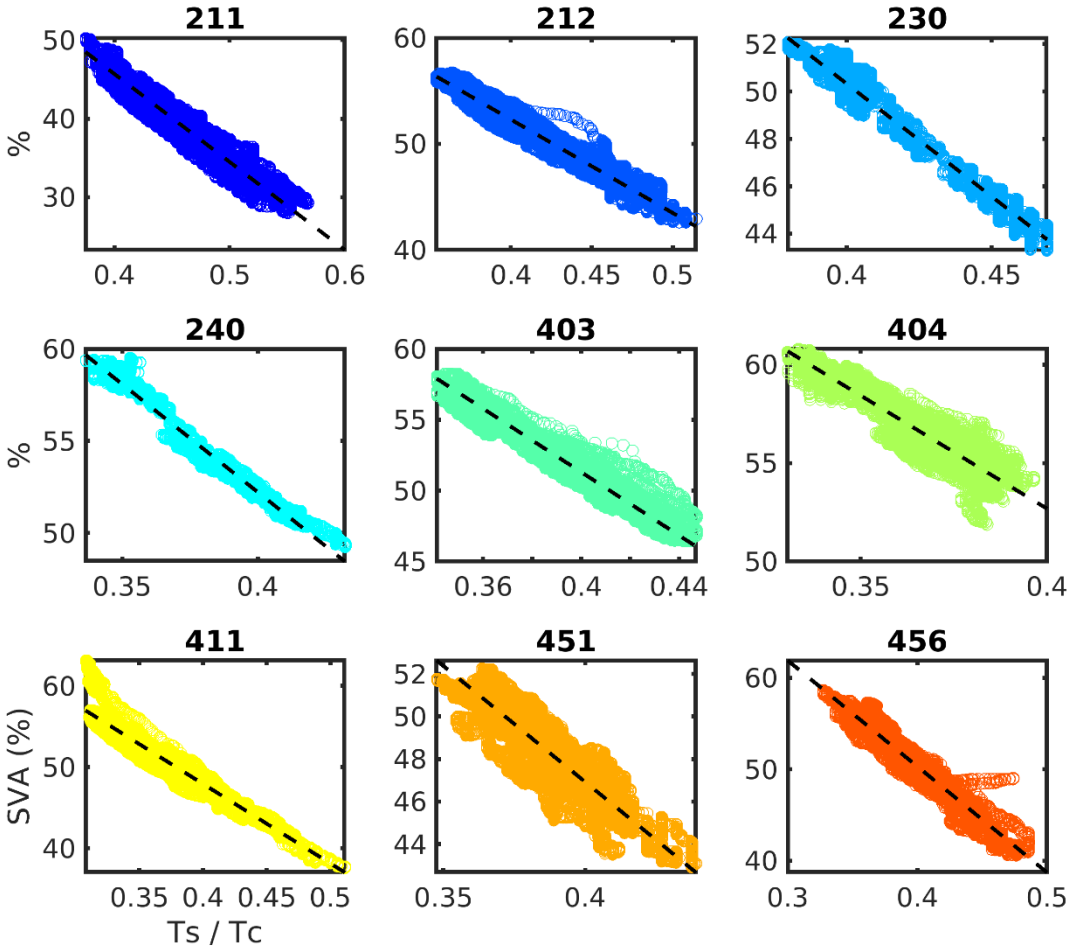

Supplementary Figure 1. Case-by-case SVA–Ts/Tc relations for nine ICU patients in the MIMIC-I data set. A significant linear relationship between SVA and Ts/Tc was discovered.

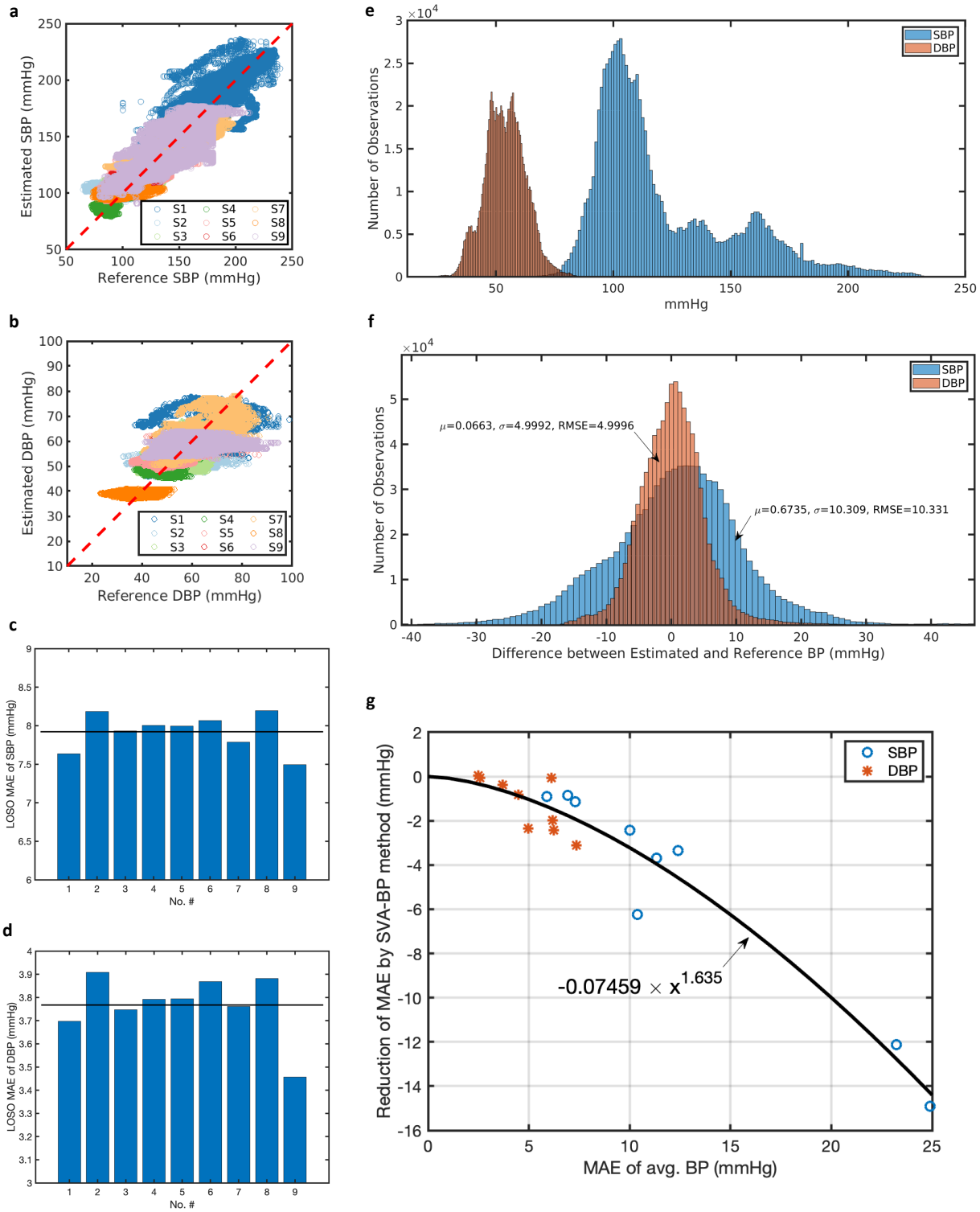

Supplementary Figure 2. SVA-BP tracking and accuracy for the MIMIC-I data set by applying Equation (4). (a) Correlation plot of the reference SBP and estimated SBP. (b) Correlation plot of the reference DBP and estimated DBP. (c) & (d) The Leave-one-subject-out (LOSO) analysis based on MIMIC-I dataset. (e) The measured SBP and DBP distributions based on MIMIC-I dataset. (f) The error distribution of SBP and DBP based on SVA-BP method in Equation (4). (g) The power decay of the estimation error when utilizing SVA-BP method.

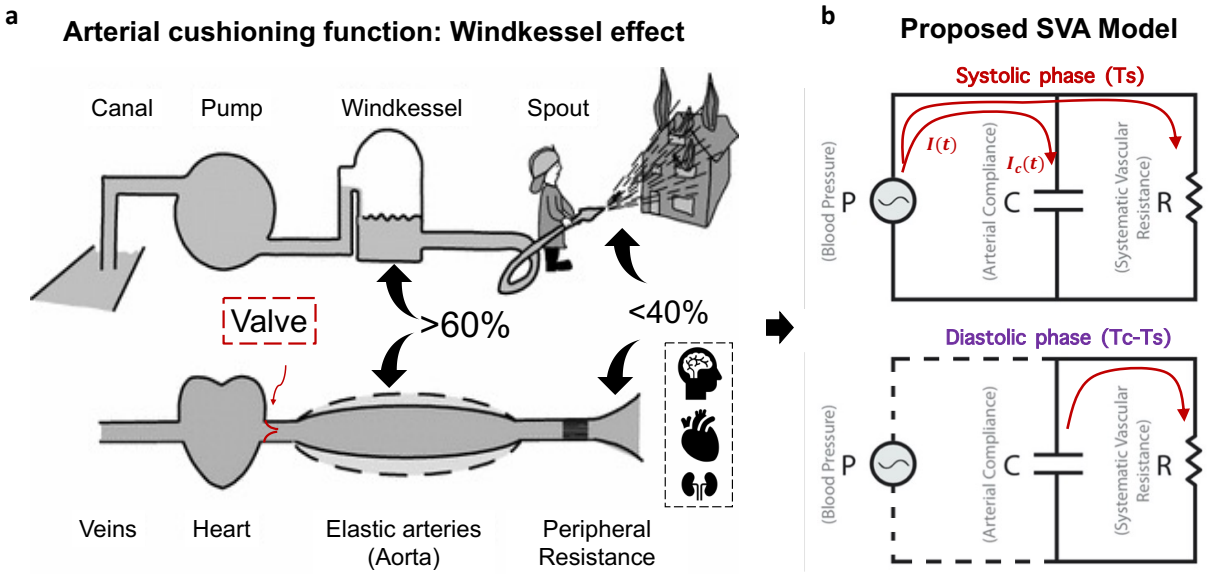

Supplementary Figure 3. Models illustrating the physical meaning of SVA in a cardiovascular system. (a) The analogy between the fire engine and the heart-to-artery system is drawn based on the Windkessel model[26]. (b) The circuit model that describes the blood flow distribution between the arterial compliance and systemic vascular resistance within a heartbeat cycle.

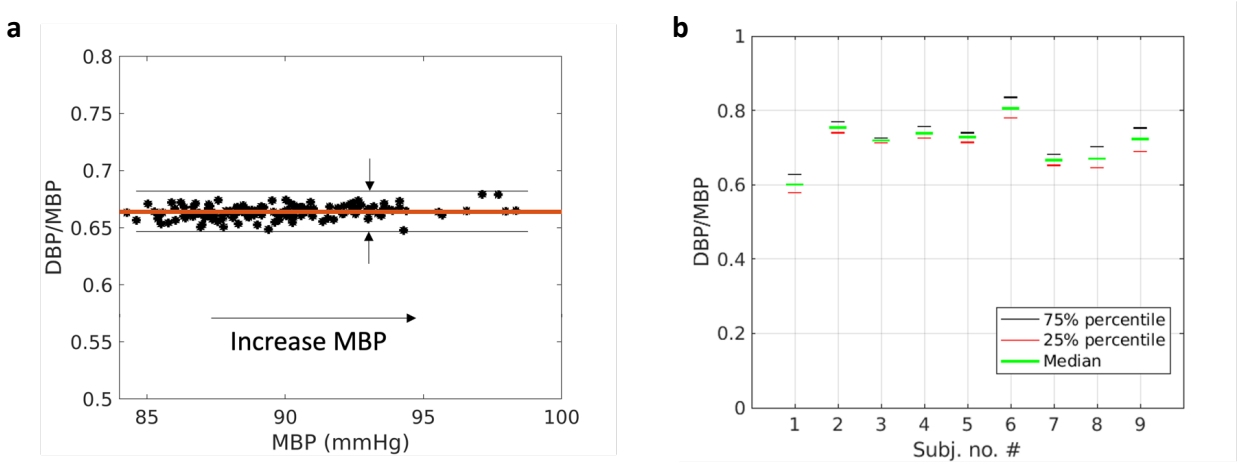

Supplementary Figure 4. Validation of the assumption "the ratio of DBP/MBP is almost a constant for each subject" for Supplementary Equation (19). Data obtained from the invasive blood pressure measurements. (a) DBP/MBP varies little with MBP, data taken from a PWH patient; (b) DBP/MBP is stable for each subject although its value varies among different subjects. Data taken from the MIMIC-I dataset.

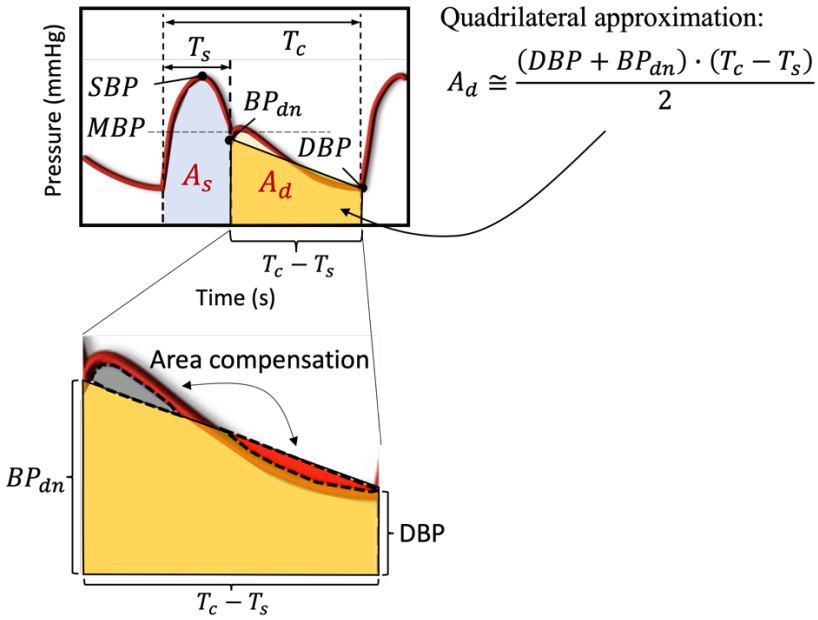

Supplementary Figure 5. The area of BP waveform in diastole is approximately described by a trapezoidal area formula.

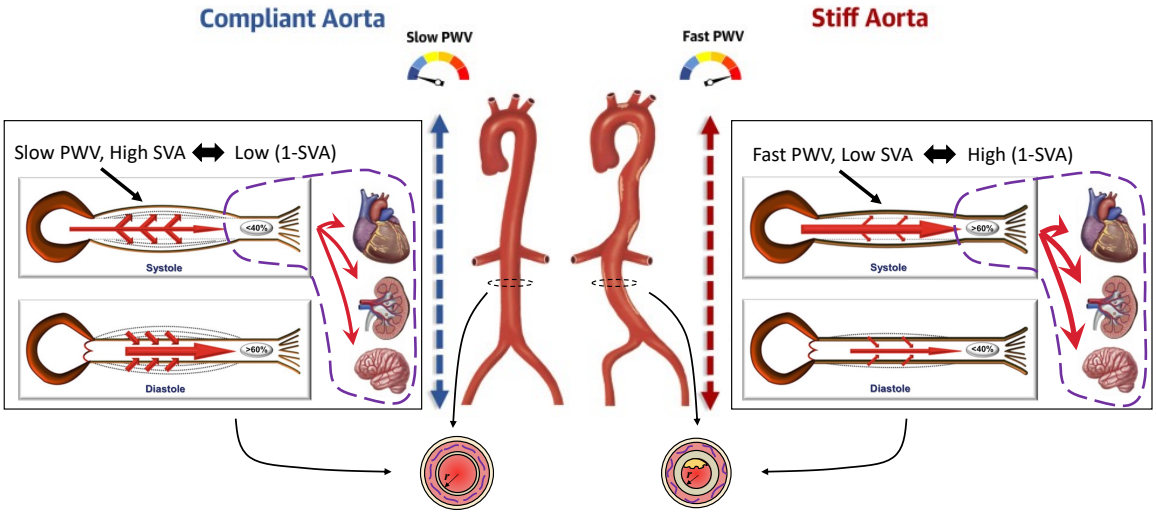

Supplementary Figure 6. The physiologic perspective on the relationship between (1-SVA) and PWV in both compliant and stiff aorta (with permissions from Ref[13,27]).

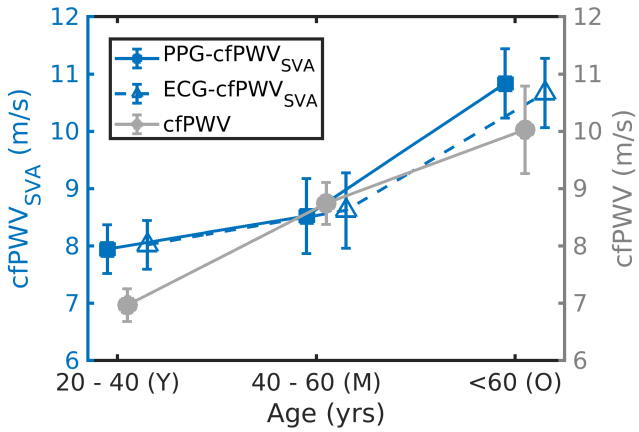

Supplementary Figure 7. Correlations of vascular ageing with transformed cfPWV by SVA and measured cfPWV. Error bars denote s.d. from the mean.

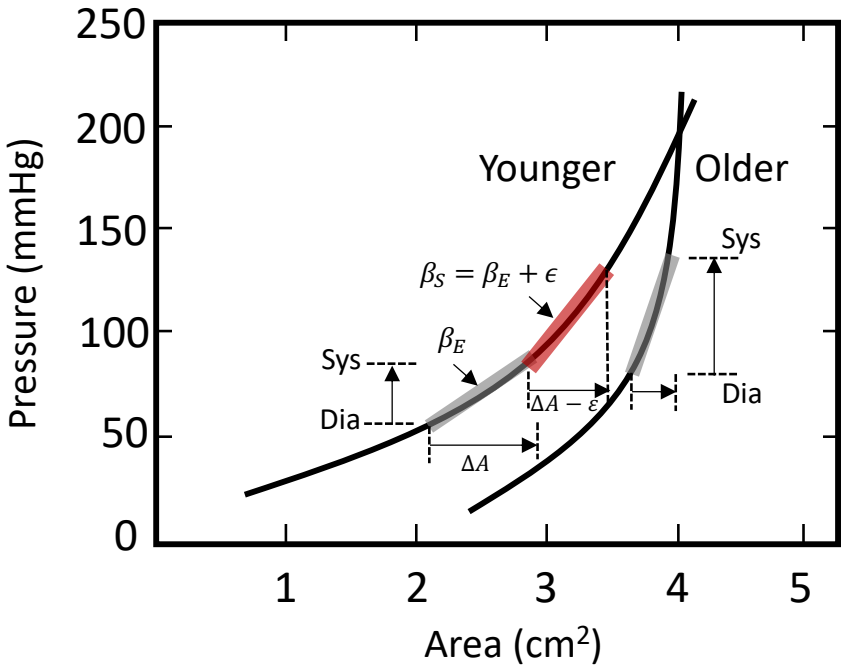

Supplementary Figure 8. Pressure and area curves in younger and older's arteries. β_E is the beta stiffness corresponding to the elastic status of artery while β_S is the beta stiffness corresponds to the stiffer status of artery for the same person. ϵ and $\varepsilon > 0$. ΔA is the pulse area difference between the systolic to diastolic phase[16].

Supplementary References:

1. B., D.P. Mechanical Properties of Arteries. *Physiol. Rev.* **58**, 397-460 (1978).
2. Fung, Y.-c. *Biomechanics: circulation* (Springer Science & Business Media, 2013).
3. Greenwald, S.E. Ageing of the conduit arteries. *J. Pathol.* **211**, 157-172 (2007).
4. B. Sonesson 1, F.H., H. Stale 3, T. Länne Compliance and diameter in the human abdominal aorta—The influence of age and sex. *Eur. J. Vasc. Endovasc.* **7**, 690-697 (1993).
5. Westerhof, N., Stergiopulos, N., Noble, M.I. & Westerhof, B.E. Cardiac Power and Ventriculo-Arterial Coupling. in *Snapshots of Hemodynamics* 135-142 (Springer, 2019).
6. Relation Between Aortic Dicrotic Notch Pressure and Mean Aortic Pressure in Adults.
7. Berne, R.M. Cardiovascular physiology. *Annu. Rev. Physiol.* **43**, 357-358 (1981).
8. Fortier, C. & Agharazii, M. Arterial Stiffness Gradient. *Pulse (Basel).* **3**, 159-166 (2016).
9. AC, B. Relation of structure to function of the tissues of the wall of blood vessels. *Physiol. Rev.* **34**, 619-642 (1954).
10. Learoyd, B.M. & Taylor, M.G. Alterations with age in the viscoelastic properties of human arterial walls. *Circ. Res.* **18**, 278-292 (1966).
11. Wilmer W. Nichols, M.F.O.R., Albert P. Avolio, Toshio Yaginuma, Joseph P. Murgo, Carl J. Pepine & C. Richard Conti Ventricular/Vascular Coupling. in *Ch 4* (Springer-Verlag New York Inc, 1987).
12. Ma, Y. et al. Relation between blood pressure and pulse wave velocity for human arteries. *PNAS.* **115**, 11144-11149 (2018).
13. Chirinos, J.A., Segers, P., Hughes, T. & Townsend, R. Large-Artery Stiffness in Health and Disease: JACC State-of-the-Art Review. *J. Am. Coll. Cardiol.* **74**, 1237-1263 (2019).
14. Gavish, B. & Izzo Jr, J.L. Arterial stiffness: going a step beyond. *Am. J. Hypertens.* **29**, 1223-1233 (2016).
15. Schultz, M.G. et al. The influence of SBP amplification on the accuracy of form-factor-derived mean arterial pressure. *J. Hypertens.* **38**, 1033-1039 (2020).
16. Gavish, B. & Izzo, J.L., Jr. Arterial Stiffness: Going a Step Beyond. *Am. J. Hypertens.* **29**, 1223-1233 (2016).
17. Mark, G.B.M.R.G. A database to support development and evaluation of intelligent intensive care monitoring. *Comput. in Cardiol.*, 657-660 (1996).
18. Bache, R.J., Yang Wang, and JOSEPH C. GREENFIELDJR. Left ventricular ejection time in valvular aortic stenosis. *Circulation.* **47**, 527–533 (1973).
19. Hasegawa M, R.D., Kinoshita Y. Timing of the Carotid Arterial Sounds in Normal Adult Men: Measurement of Left Ventricular Ejection, Pre-Ejection Period and Pulse Transmission Time. *Cardiology.* **78**, 138-149 (1991).
20. Luomanmaki, K. & Heikkila, J. Estimation of the severity of aortic incompetence from prolongation of the left ventricular ejection time. *Acta Med. Scand.* **1-2**, 107-114 (1970).
21. London G. et al. Increased systolic pressure in chronic uremia. Role of arterial wave reflections. *Hypertension.* **20**, 10-19 (1992).
22. London, G.M. et al. Cardiac and arterial interactions in end-stage renal disease. *Kidney Int.* **50**, 600-608 (1996).
23. London G M et al. Cardiac hypertrophy, aortic compliance, peripheral resistance, and wave reflection in end-stage renal disease. Comparative effects of ACE inhibition and calcium channel blockade. *Circulation.* **90**, 2786-2796 (1994).

24. London, G.M. Influence of sex on arterial hemodynamics and blood pressure. *Hypertension.* **26**, 514-519 (1995).
25. London, G.M., Pannier, B. & Safar, M.E. Arterial Stiffness Gradient, Systemic Reflection Coefficient, and Pulsatile Pressure Wave Transmission in Essential Hypertension. *Hypertension.* **74**, 1366-1372 (2019).
26. Westerhof, N., Lankhaar, J.W. & Westerhof, B.E. The arterial Windkessel. *Med. Biol. Eng. Comput.* **47**, 131-141 (2009).
27. Salvi, P. Pulse waves. *How vascular hemodynamics affects Blood pressure.* (Springer, 2017).